

Phase transition and anomalous electronic behavior in the layered superconductor CuS probed by NQR

R. R. Gainov,^{1,*} A. V. Dooglav,¹ I. N. Pen'kov,² I. R. Mukhamedshin,^{1,3} N. N. Mozgova,⁴
I. A. Evlampiev,¹ and I. A. Bryzgalov⁵

¹*Department of Physics, Magnetic Radiospectroscopy Laboratory, Kazan State University, Kremlevskaya Str. 18, 420008 Kazan, Russian Federation*

²*Department of Geology, Kazan State University, Kremlevskaya Str. 4/5, 420111 Kazan, Russian Federation*

³*Laboratoire de Physique des Solides, UMR 8502, Universite Paris-Sud, 91405 Orsay, France*

⁴*Institute of Geology of Ore Deposits, Petrography, Mineralogy and Geochemistry, Russian Academy of Science, Staromonetny Per. 35, Moscow 119017, Russian Federation*

⁵*Department of Geology, Moscow State University, Vorob'evy Gory, Moscow 119991, Russian Federation*

(Received 11 June 2008; revised manuscript received 28 November 2008; published 17 February 2009)

Nuclear quadrupole resonance (NQR) on copper nuclei has been applied for studies of the electronic properties of quasi-two-dimensional (2D) low-temperature superconductor CuS (covellite) in the temperature range of 1.47–290 K. Two NQR signals corresponding to two structural nonequivalent sites of copper, Cu(1) and Cu(2), have been found. The temperature dependences of copper quadrupole frequencies, linewidths, and spin-lattice relaxation rates altogether demonstrate the structural phase transition near 55 K, which is accompanied by transformations of the electronic spectrum not typical for simple metals. The analysis of NQR results and their comparison with literature data show that the valence of copper ions at both sites is intermediate between monovalent and divalent states with the dominance of the former. It has been found that there is a strong hybridization of the Cu(1) and Cu(2) conduction bands at low temperatures, indicating that the charge delocalization between these ions takes place even in 2D regime. On the basis of our data, the occurrence of an energy gap, charge fluctuations, and charge-density waves, as well as the nature of the phase transition in CuS, are discussed. It is concluded that some physical properties of CuS are similar to those of high-temperature superconductors in the normal state.

DOI: [10.1103/PhysRevB.79.075115](https://doi.org/10.1103/PhysRevB.79.075115)

PACS number(s): 74.70.Ad, 71.28.+d, 76.60.Gv, 91.60.Pn

I. INTRODUCTION

Metallic chalcogenides exhibit a fascinating variety in crystal-chemistry and physical properties of both scientific interest and practical applications.^{1–4} A role of copper binary chalcogenide CuS (referred to as covellite or covelline) should be specially emphasized. This compound is widely used in optoelectronic devices⁵ and has been extensively studied due to possible applications in the synthesis of composite high-temperature superconductors (HTSCs),⁶ as a cathode material in rechargeable batteries,⁷ and in the creation of nanotechnological products.⁸ From a scientific point of view, CuS has drawn significant interest as a superconductor.^{9–11} One of the pronounced features of CuS is the occurrence of quasi-two-dimensional (2D) layered structure, which is built up of the triangular unit CuS₃ (Fig. 1) to some extent similar to those in Cu-oxide HTSCs (constructed from CuO₄ layers). Since after the discovery of HTSC,¹² the nature of superconductivity (SC) in these materials is still unclear; some researchers suggest studying the relationship of SC mechanisms through an analogy between Cu-O and either Co-O bonds in Co-oxide SCs (Ref. 13) or Cu-S bonds in CuS.^{14,15} It has been also found that HTSC in the normal state and transition-metal dichalcogenides (CuS₂, NbS₂, Mo_xW_{1-x}Se₂, and others) exhibits some general and hard-to-explain electronic features [energy gaps and charge-density waves (CDWs)], which are expedient to study on the basis of common views.^{16–20} Finally, CuS by itself possesses a set of indistinguishable features in the crystal chemistry, in

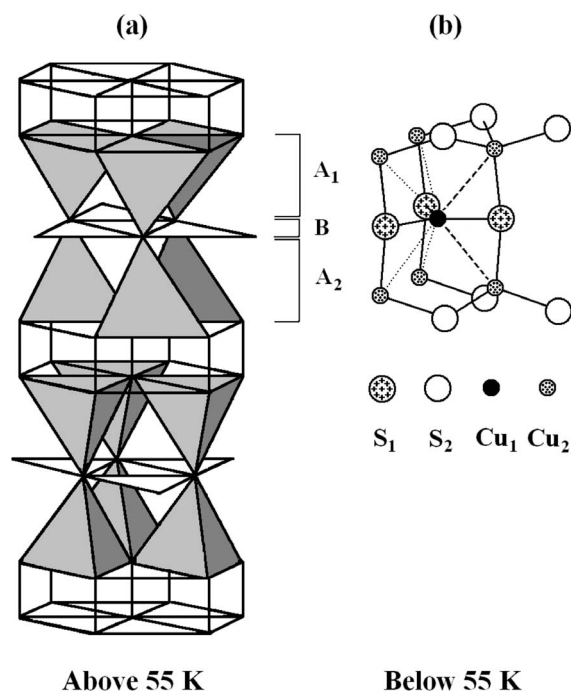


FIG. 1. (a) Crystal structure of the covellite CuS above $T_{PT} = 55$ K (reproduced from Ref. 30). The main structural units are the Cu(1)S₃ triangles (layer B) and the Cu(2)S₄ tetrahedra (layers A₁ and A₂). (b) The fragment of crystal structure of CuS below $T_{PT} = 55$ K (reproduced from Ref. 24). It is clearly seen that the Cu(2)S₄ tetrahedra are distorted. For details, see Sec. II.

TABLE I. Interatomic distances and bond angles in covellite CuS above and below the temperature of phase transition ($T_{PT}=55$ K).

	Hexagonal symmetry, 295 K				Orthorhombic symmetry, 8 K
	Ref. 29	Ref. 32	Ref. 21	Ref. 33	Ref. 24
					$2 \times 2, 18(2)$ Å;
Cu(1)-S(1)-S(1)	$3 \times 2, 19$ Å	$3 \times 2, 195(5)$ Å	$3 \times 2, 1905(2)$ Å	$3 \times 2, 1915(4)$ Å	$1 \times 2, 17(2)$
					$1 \times 2, 328(4)$;
Cu(2)-S(1)-S(2)-S(2)	$1 \times 2, 34$;	$1 \times 2, 334(6)$;	$1 \times 2, 331(2)$;	$1 \times 2, 339(2)$;	$1 \times 2, 32(2)$;
	$3 \times 2, 30$	$3 \times 2, 312(4)$	$3 \times 2, 305(2)$	$3 \times 2, 305(1)$	$2 \times 2, 281(8)$
S(2)-S(2)	$1 \times 2, 09$	$1 \times 2, 037(11)$	$1 \times 2, 071(4)$	$1 \times 2, 086(7)$	$1 \times 2, 03(2)$
					$1 \times 3, 260(5)$;
Cu(1)-Cu(2)	$3 \times 3, 21$		$3 \times 3, 199(4)$		$2 \times 3, 044(7)$
					$1 \times 3, 642$ ^a ;
S(1)-S(2)	$3 \times 3, 75$	$3 \times 3, 773(9)$		$3 \times 3, 754$ ^a	$2 \times 3, 793$ ^a
S(1)-Cu(2)-S(2)	107°	$108, 6(3)^\circ$	$108, 16(7)^\circ$	$108, 04(8)^\circ$	
S(2)-Cu(2)-S(2)	111	110,3(3)	110,76(7)	110,87(8)	
S(1)-Cu(1)-S(1)		119,7(3)			
S(1)-S(1)-S(1)		120,0(0)			
Cu(2)-S(1)-Cu(2)					170°

^aThe values were calculated by Ref. 25 on the basis of data from corresponding references.

particular, undetermined valence state of copper,^{21–23} the character of the low- T phase transition (PT),^{24,25} an anomalous negative Knight shift,¹⁵ etc. In any case, the clarification of the problems mentioned requires the study of local properties of CuS, for which nuclear resonance methods are most suitable.

In this paper, we report the results of nuclear quadrupole resonance (NQR) measurements including the ^{63}Cu quadrupole frequencies, linewidths, and Cu spin-lattice relaxation rates in synthetic and natural samples of CuS in the T range of 1.47–290 K. The single ^{63}Cu NQR signal in CuS was first observed by Abdullin *et al.*²⁶ at about 14.88 MHz but only at 4.2 and 77 K. Later Itoh *et al.*²⁷ and Tnabe *et al.*²⁸ extended this study by measurements of the T dependences of the NQR frequency and nuclear relaxation²⁷ above 4.2 K. In addition, from NMR spectra Itoh *et al.*²⁷ supposed the existence of another ^{63}Cu NQR signal at about 1.5 MHz above the temperature of the structural phase transition $T_{PT}=55$ K. In contrast, the NMR studies of Saito *et al.*¹⁵ predicted the occurrence of this NQR signal not only above but also below T_{PT} at about 1.8 MHz. In order to specify the low- T features of the CuS electronic structure and resolve the opposing data, we have thoroughly re-examined the T dependences of Cu spectroscopic and relaxation parameters. In particular, below T_{PT} we have experimentally found the low-frequency ^{63}Cu NQR signal at 1.87 MHz (4.2 K) and have studied its nuclear relaxation $T_1(T)$; we have revealed the change in the character of the ^{63}Cu NQR linewidth $\Delta\nu_Q$ broadening of high-frequency signal and rapid divergence of $^{63}\text{Cu}T_1T$ from its constant behavior typical for majority of metals. On the basis of the experimental data obtained, some aspects of the CuS crystal structure and its physical properties are presented and discussed.

II. CRYSTAL-CHEMISTRY AND ELECTRONIC PROPERTIES

The crystal structure of CuS has been described in numerous papers.^{21,29–35} The elementary cell of CuS at room T has a hexagonal symmetry corresponding to the space group $P6_3/mmc$ with 6 f.u./unit cell. The structure of CuS can be described as a “sandwich,” which consists of three alternating layers A_1 - B - A_2 (Fig. 1). The layer B represents the net of $[\text{Cu}(1)\text{-S}(1)_3]$ triangles combined by vertices. The layers A_1 and A_2 are made up of $[\text{Cu}(2)\text{-S}(1)\text{S}(2)_3]$ tetrahedra which are turned in opposite directions. The units A_1 - B - A_2 are connected together along the c axis by S(2)-S(2) bonds (“dumbbells”). In Table I, the interatomic distances and angles between the chemical bonds in CuS are reported. It is noted that the Cu(1)-S(1) bonds (about 2.19 Å) are strikingly shorter than the Cu-S bonds in triangular units for majority of other copper sulfides (about 2.33 Å).^{21,33} This fact strongly suggests that the Cu(1)-S(1) bond strength should be very large.³³ It was found also that Cu(1) ions in the $[\text{Cu}(1)\text{-S}(1)_3]$ triangles have a large thermal motion along the c axis.²¹

Covellite CuS represents the metal with excellent hole conductivity,⁴ which becomes superconducting below T_C ranging from 1.72 K (Ref. 15) down to 1.31 K.¹⁰ Recent studies show that CuS is attributed to the class I SC materials¹¹ and might be an anisotropic SC.³⁶ It is interesting that CuS is the first specimen of natural solids (minerals), in which the SC transition was detected.¹¹

The heat-capacity studies revealed that there is an anomaly around 55 K and that the capacity is proportional to T^2 in the region of 5–20 K.³⁷ This T^2 law was explained by the Debye theory of low-frequency modes of the lattice vi-

brations with the assumption of a 2D lattice, which is probably caused by weak bonding in the c -axis direction. At temperatures above 50 K the lattice heat capacity was estimated in terms of a three-dimensional (3D) model. The gradual transformation from the 3D to 2D lattice of CuS with decreasing T is indirectly confirmed by theoretical calculations²⁵ and experimental studies of the electrical conductivity¹⁵ and Cu spin-lattice relaxation.²⁷

The T dependences of x ray^{24,38} and neutron diffraction²⁴ revealed the second-order PT at about $T_{PT}=55$ K to a phase with the orthorhombic symmetry and space group $Cmcm$. Later the occurrence of the second-order PT was verified through the electric resistivity,¹⁴ Hall coefficient,¹⁴ and Raman spectroscopy³⁹ measurements. This PT can be visualized as a shift of the layers formed by Cu(1)S₃ triangles with respect to the Cu(2)S₄ layers perpendicular to the c axis with the change in the Cu(2)-S(1)-Cu(2) bonding angle from 180° at room T to 170° below T_{PT} (Fig. 1).²⁴ This distortion involves slight but important changes in the Cu(1) and Cu(2) bond lengths (Table I). It was assumed that the formation of the metallic Cu(1)-Cu(2) bond (3.04 Å) is a driving force for the PT (Ref. 24); however, theorists proposed that the PT is caused by van der Waals interactions of the S(1)-S(2) contacts (3.64 Å).²⁵ Another possibility is that the change in the bonding nature of the S(2)-S(2) or Cu(2)-S(1) pairs on varying T may stimulate the PT.³⁸

Another important problem still lacking clarity is the active valence states of copper and sulfur—their distribution in the crystal structure of CuS. In particular, the (Cu²⁺)(S₂²⁻)(Cu₂¹⁺)(S²⁻) valence formalism was proposed,^{30,31,40-42} i.e., both valence forms of copper present in the system under study. However, electron paramagnetic resonance (EPR) studies in CuS showed no signal of paramagnetic Cu²⁺ at room and low temperatures.²³ Some measurements by x-ray photoelectron spectroscopy (XPS) and x-ray absorption spectroscopy (XAS) (Refs. 43–49) point out that covellite CuS is better described as a compound consisting of only Cu¹⁺. Other XPS,^{44,50} x-ray emission spectroscopy (XES),⁵⁰ and x-ray absorption near-edge spectroscopy (XANES) (Ref. 51) studies revealed the presence of two different electronic states of the S atoms. Therefore, the bonding was described as (Cu¹⁺)₃(S₂⁻²)(S⁻¹) (Ref. 24) or (Cu¹⁺)₃(S₂⁻¹)(S⁻²) (Ref. 25) in terms of the ionic model. At the same time, other crystal-chemical and theoretical studies pointed that Cu possesses a valence state, which is intermediate between Cu¹⁺ and Cu²⁺.²¹⁻²³ Some magnetic-susceptibility measurements of CuS show the existence of the magnetic moment μ_{eff} of about $0.28\mu_B$.²⁴ However, the results of recent studies provide no evidence for such behavior.^{14,27} The fluorescent XES investigations show that the band of CuS is composed of three parts, constituted mainly by Cu-3*d*, S-3*p*, and (to a less extent) S-3*s* orbitals.⁵²

III. MATERIALS AND EXPERIMENTAL METHODS

We have studied two samples. Sample 1 is synthetic and has been prepared by a solid-phase reaction of high-purity elements Cu and S. Amounts of Cu and S were taken in relations corresponding to the composition of stoichiometric

covellite Cu_{1.00}S_{1.00}. The synthesis was carried out in a sealed quartz tube evacuated down to the residual pressure of 10⁻¹ Pa. The regime of preparation was the following: heating at 480 °C for one week and gradual cooling during 2 h. The synthetic sample had a dark-blue color. The sample 2 is a natural covellite, originating from the Bor copper-ore deposit (Serbia). This sample consisted of large (up to 1.5 cm) crystallites in the form of thin plates and had a playing indigo-blue color with varnish glitter.

The electron-probe microanalyses (EPMA) carried out by scanning microscope Camebax SX-50 confirmed the chemical composition of sample 1 and showed that the composition of sample 2 is close to stoichiometric Cu_{0.99}S_{1.00}. The phase homogeneity and CuS structure for both samples were confirmed by x-ray diffractometry.

The copper NQR measurements were carried out on standard home-built coherent pulsed NMR/NQR spectrometers. For better penetration of the high-frequency magnetic field all samples were crushed in an agate mortar to a particle size smaller than 75 μm and packed in epoxy resin “Stycast 1266.” NQR spectra were taken “point by point” after the $\pi/2$ - π pulse sequence in the frequency sweep mode; after that the detailed NQR spectra were created according to the Fourier mapping algorithm.⁵³ The Cu nuclear spin-lattice relaxation time T_1 was measured at the peak of the ⁶³Cu NQR signal and calculated by plotting the Cu nuclear spin-echo intensity as a function of the time delay Δt between the saturating and $\pi/2$ - π probing pulses.

IV. NMR-NQR BACKGROUND

The nuclear spins I interact with their electronic environment through quadrupole (i.e., electric) and magnetic hyperfine couplings.^{54,55} In general, the NMR spectrum of a quadrupole nucleus (i.e., nucleus with spin $I > \frac{1}{2}$) is described by the following spin Hamiltonian:

$$H = H_Z + H_Q + H_M. \quad (1)$$

The term H_Z is the Zeeman interaction of nuclear magnetic moments having the gyromagnetic ratio γ_n with the applied external magnetic field H_0 ,

$$H_Z = -\gamma_n \hbar H_0 I. \quad (2)$$

The term H_Q refers to the coupling of the nuclear quadrupole moment eQ to the local crystal electric field gradient (EFG),

$$H_Q = \frac{eQV_{ZZ}}{4I(2I-1)} \left\{ 3I_z^2 - I(I+1) + \frac{1}{2} \eta(I_+^2 + I_-^2) \right\}, \quad (3)$$

where V_{ZZ} is the largest component of the crystal EFG tensor and $\eta = |V_{XX} - V_{YY}| / V_{ZZ}$ is the asymmetry parameter showing the deviation of the EFG symmetry from the axial one.

The term H_M is the interaction of a nuclear spin I with static and time-dependent parts of the local hyperfine magnetic field generated by conduction carriers. The static part gives rise to a well-known Knight shift $K = \Delta H / H_0$ of the NMR line, whereas the fluctuating part is the source of the nuclear spin-lattice relaxation.

TABLE II. The magnitudes of asymmetry parameter η in covellite CuS above and below the temperature of phase transition ($T_{PT} = 55$ K).

	$T > T_{PT}$		$T < T_{PT}$	
	Ref. 27	Ref. 15	Ref. 27	Ref. 15
Triangular units [Cu(1)-S(1) ₃], η (a.u.)	~0 (100 K)			
Tetrahedral units [Cu(2)-S(2) ₃ S(1)], η (a.u.)	~0 (100 K)	0? (60 K)	$\neq 0$ and/or $\nu_Q \ll 1.5$ MHz (35 K)	0.50–0.55 (15 K)

The pure NQR spectrum is observed in the absence of the external ($H_0=0$) and internal ($H_{int}=0$) static magnetic fields. The number of copper NQR lines is determined by two different isotopes (^{63}Cu , $I=3/2$, 69.2% natural abundance, $\gamma/2\pi=1.128$ kHz/Oe, and $Q=-0.22$ barn; ^{65}Cu , $I=3/2$, 30.8% natural abundance, $\gamma/2\pi=1.209$ kHz/Oe, and $Q=-0.204$ barn) and by an amount of crystallographically nonequivalent positions of copper in the crystal structure. So, each nonequivalent position should give two NQR lines, one for each isotope, with frequencies

$${}^{63,65}\nu_Q = \frac{e^{63,65} Q V_{ZZ}}{2h} \sqrt{1 + \frac{1}{3} \eta^2}. \quad (4)$$

It should be noted that besides the quadrupole moment eQ of the nucleus the NQR frequency, ν_Q , depends on a certain arrangement of the surrounding ions through the parameters V_{ZZ} and η . The values of η for the triangular (plane) Cu(1) and tetrahedral Cu(2) sites in covellite CuS are given in Table II.

In a semiempirical approach, it is assumed that components of the EFG tensor at Cu nuclei sites can be written as the sum of two terms—lattice and valence contributions,

$$V_{ZZ} = (1 - \gamma_\infty) V_{\text{latt}} + (1 - R_{\text{val}}) V_{\text{val}}. \quad (5)$$

The parameters γ_∞ and R_{val} are the Sternheimer antishielding factors. The first contribution arises from all ion charges outside the ion under consideration and can be calculated in a straightforward manner using the model of point charges (MPCs),

$$V_{\text{latt}} = \sum_i \frac{q_i (3 \cos^2 \theta_i - 1)}{r_i^3}, \quad (6)$$

where q_i and r_i are the charge and the position of the i th ion, respectively; θ_i is the angle between the z axis of the EFG tensor and the direction to the neighboring ion.

The second term in Eq. (5) arises from unfilled $3d$ and $4p$ shells and nonspherical distortions of inner orbitals of the Cu ion. Taking into account only holes in the Cu orbitals, the contributions of $3d$ and $4p$ shells can be written as⁵⁶

$$V_{\text{val}}^{(3d)} = -\frac{4}{7} e \langle r^{-3} \rangle_{3d} \left[N_{3d(3z^2-r^2)} - N_{3d(x^2-y^2)} - N_{3d(xy)} + \frac{1}{2} N_{3d(xz)} + \frac{1}{2} N_{3d(yz)} \right], \quad (7a)$$

$$V_{\text{val}}^{(4p)} = -\frac{4}{5} e \langle r^{-3} \rangle_{4p} \left[N_{4p(z)} - \frac{1}{2} N_{4p(x)} - \frac{1}{2} N_{4p(y)} \right], \quad (7b)$$

where $N_{3d(x,y,z)}$ and $N_{4p(x,y,z)}$ are the numbers of electronic holes in different $3d$ and $4p$ orbitals, and the charge of an electron is given by $-e$. The comparison of ν_Q and V_{ZZ} deduced from theoretical calculations for different structural models [Eq. (5)] with experimental values [Eq. (4)] allows one to determine individual features of the local electronic arrangement and features of chemical bonds.

The nuclear spin-lattice relaxation rate depends on specific sources of the field fluctuations in crystal structures. Therefore, studies of the temperature dependences of the nuclear relaxation often allow sensing the lattice dynamics and transport properties of the material.

V. RESULTS

A. Cu NQR spectra

It was found that the copper NQR spectrum of the synthetic sample of CuS (sample 1) at 4.2 K consists of two copper doublets (i.e., the ^{63}Cu and ^{65}Cu isotope lines) at 14.88 and 13.77 MHz (“high-frequency” doublet, Fig. 2) and at 1.87 and 1.73 MHz (“low-frequency” doublet, Fig. 3). The ^{63}Cu and ^{65}Cu spectrum lines are identified from the ratios of

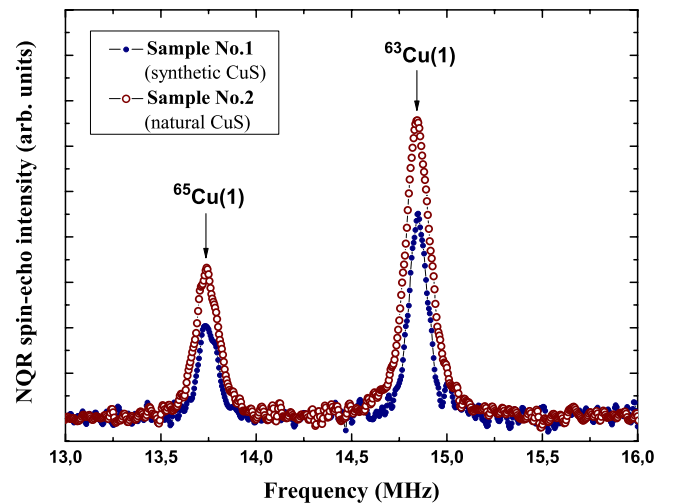


FIG. 2. (Color online) High-frequency copper NQR spectra for sample 1 (closed blue circles) and sample 2 (opened red circles) at 4.2 K. Arrows point to the positions of $^{63}\text{Cu}(1)$ and $^{65}\text{Cu}(1)$ NQR signals. Curves are guides for the eyes. For details, see Secs. V A and VI A.

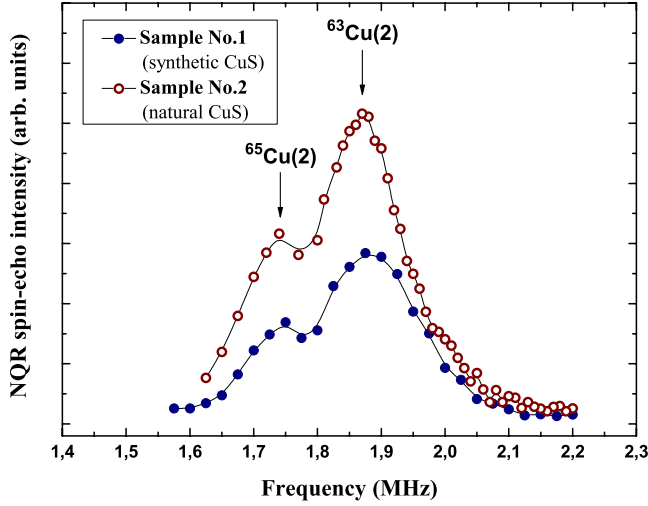


FIG. 3. (Color online) Low-frequency copper NQR spectra for sample 1 (closed blue circles) and sample 2 (opened red circles) at 4.2 K. Arrows point to the positions of $^{63}\text{Cu}(2)$ and $^{65}\text{Cu}(2)$ NQR signals. Curves are guides for the eyes. For details, see Secs. V A and VI A.

isotope quadrupole moments ($^{63}\text{Q}/^{65}\text{Q}=1.081$) and their natural abundance ($^{65}\text{A}/^{63}\text{A}=0.45$). The NQR spectrum of the natural sample of CuS (sample 2) is similar to that for sample 1 (Figs. 2 and 3). The presence of two spectral lines for both copper isotopes allows us to attribute the NQR spectra to the two crystallographically nonequivalent sites of copper nuclei in CuS.

B. Temperature dependence of Cu NQR frequencies and linewidths

The dependence of the high-frequency ^{63}Cu NQR line position on T is shown in Fig. 4(a). In general, the quadrupole frequency ν_Q decreases with increasing temperature without significant anomalies. However, we focus here on two weak effects: the change in the slope in the T dependence of ν_Q at 65 K (i.e., near T_{PT}) and 210 K. We mention here that the same effect has been clearly seen at about 65 K in earlier studies.^{27,28,57} In order to describe an approximate behavior of ν_Q in the region of 65–290 K we applied the following equation:⁵⁴

$$\nu_Q(T) = \nu_Q(0)(1 - aT^b), \quad (8)$$

where $\nu_Q(0)$, a , and b are the fitting parameters. The best result of fitting depicted in Fig. 4(a) by solid curve was obtained for $\nu_Q(0)=(14.95 \pm 0.02)$ MHz, $a=(1.7 \pm 0.5) \times 10^{-4}$ MHz/K, and $b=(0.98 \pm 0.05)$. On the other hand, in the range of 65–290 K the $\nu_Q(T)$ dependence can be divided into two regions, both described by Eq. (8) with $b=1$, i.e., by a linear function. The results of these fits were obtained for $\nu_Q(0)=(14.96 \pm 0.01)$ MHz, $a=(1.61 \pm 0.02) \times 10^{-4}$ MHz/K (in the range of 65–210 K) and $\nu_Q(0)=(14.90 \pm 0.01)$ MHz, $a=(1.42 \pm 0.02) \times 10^{-4}$ MHz/K (210–290 K) [shown in the inset of Fig. 4(a)].

The Cu NQR line shape was well fitted by a Lorentzian function at all temperatures studied and its linewidth was

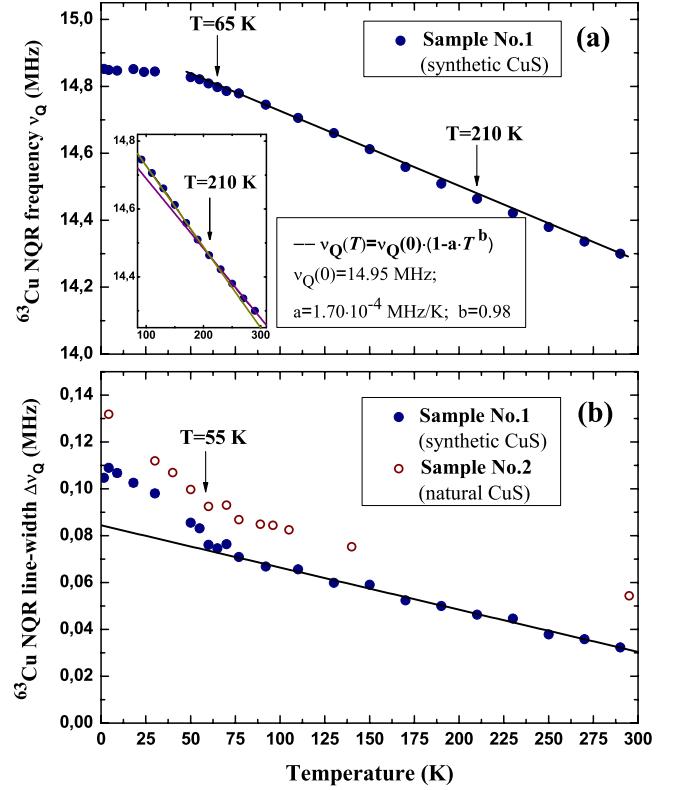


FIG. 4. (Color online) (a) Temperature dependence of $^{63}\text{Cu}(1)$ NQR frequency ν_Q for sample 1 (closed blue circles) with the fit of data by Eq. (8) within 65–290 K (solid curve) and extracted fitting parameters. Arrows point to the positions of the change in slope in the $\nu_Q(T)$ dependence at 210 and at 65 K. Inset of (a) shows that the $\nu_Q(T)$ dependence can be described by two linear functions in the ranges of 65–210 K and 210–290 K. (b) Temperature dependences of $^{63}\text{Cu}(1)$ NQR linewidths for sample 1 (blue closed circles) and sample 2 (red opened circles). Arrow points to the temperature 55 K, below which the strong broadening starts up. The solid line is the fit by the linear function within 55–290 K. For details, see Secs. V B and VI D.

taken as a full width at half maximum (FWHM). The T dependence of $\Delta\nu_Q$ is displayed in Fig. 4(b). As one can see, the NQR linewidth increases linearly with decreasing T in the range of 290–55 K, but the line broadens drastically below 55 K. It is noteworthy that comparison with synthetic CuS (sample 1) natural CuS (sample 2) exhibits identical T dependence of the quadrupole frequency ν_Q (hence not shown); however, the NQR linewidth $\Delta\nu_Q$ is broader by an additive constant of about 15–20 kHz in the whole T region, which is obviously caused by lattice defects in natural CuS with respect to the synthetic analog [Fig. 4(b)].

Due to technical limitations, our NQR spectrometer cannot be used at frequencies below about 1.5 MHz. Since ν_Q of the low-frequency doublet decreases at higher temperatures, the T dependences of ^{63}Cu ν_Q and $\Delta\nu_Q$ have been studied only up to 30 K. Within an experimental accuracy the values of ν_Q and $\Delta\nu_Q$ of the low-frequency ^{63}Cu NQR signal changes, respectively, from 1.87 MHz and 150 kHz at 4.2 K down to 1.78 MHz and 120 kHz at 30 K. The ^{65}Cu NQR line is about 1.1 times narrower than that of ^{63}Cu for both posi-

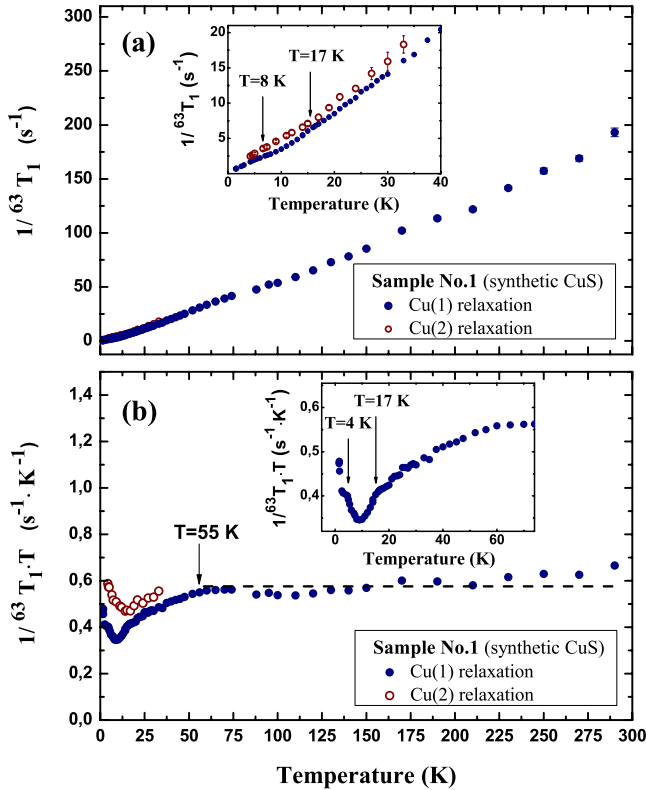


FIG. 5. (Color online) (a) Temperature dependence of nuclear spin-lattice relaxation T_1^{-1} for $^{63}\text{Cu}(1)$ in sample 1 (blue closed circles). Inset of (a) shows the $T_1^{-1}(T)$ dependences for $^{63}\text{Cu}(1)$ and $^{63}\text{Cu}(2)$ within the range of 1.47–40 K (blue closed and opened circles, respectively). Arrows point to the positions of bends in $T_1^{-1}(T)$ at about 17 and 8 K. (b) Temperature dependences of $(T_1 T)^{-1}$ for $^{63}\text{Cu}(1)$ and $^{63}\text{Cu}(2)$ in sample 1 (closed and opened circles, respectively). Arrow points to the temperature 55 K, above which the constant behavior of $(T_1 T)^{-1}$ holds approximately (dashed line) and below which the anomalous behavior of relaxation starts up. Inset of (b) shows the $(T_1 T)^{-1}$ dependence for $^{63}\text{Cu}(1)$ within the range of 1.47–74 K; arrows point to the positions of bends in $(T_1 T)^{-1}$ at about 17 and 4 K. For details, see Secs. VC and VIC.

tions of copper in all studied T regions; this states the quadrupole mechanism of the Cu NQR line broadening.

C. Temperature dependence of nuclear spin-lattice relaxation rates

The longitudinal magnetization recovery curves for Cu in both samples were well fitted to a single exponential function $[M(\infty) - M(\Delta t)]/M(\infty) = \exp[-(\Delta t/T_1)]$. The T dependences of the ^{63}Cu nuclear spin-lattice relaxation rates $1/^{63}T_1$ and $1/^{63}T_1 T$ for both positions of copper in sample 1 are presented in Fig. 5.

The relaxation rate $1/^{63}T_1$ of Cu nuclei, corresponding to the high-frequency NQR line, linearly increases with increasing T [Fig. 5(a)]. However, more detailed measurements at low T revealed the change in the slope in the T dependence of $1/^{63}T_1$ at about 17 and 8 K [inset of Fig. 5(a)]. The $1/^{63}T_1 T$ exhibits a T -independent behavior between 290 K

and $T_{PT}=55$ K, but below T_{PT} it demonstrates a strong falling down with the minimum at 8–9 K and with the change in slope at 17 K [Fig. 5(b)]. In contrast, in the region of 7–1.47 K the $1/^{63}T_1 T$ shows an abrupt increasing, and additionally, near 4 K the bend of the T dependence of $^{63}T_1 T$ is observed [inset of Fig. 5(b)].

Remarkably, the values of $1/^{63}T_1$ and $1/^{63}T_1 T$ for Cu nuclei, corresponding to the low-frequency NQR line, show the T dependence very similar to that of high-frequency Cu (Fig. 5). Nevertheless, there are two differences. First, it is clearly seen that in the studied T region the low-frequency ^{63}Cu nuclei are relaxing about 1.2 times faster than those of high-frequency ^{63}Cu [inset of Fig. 5(a)]. Second, the minimum in $1/^{63}T_1 T$ occurs at higher T near 16 K.

The isotopic ratio of $T_1^{-1}(^{65}\text{Cu})/T_1^{-1}(^{63}\text{Cu})$ can be used to identify the nature of the relaxation process.⁵⁸ In case of CuS, we have found that at all temperatures the value of $T_1^{-1}(^{65}\text{Cu})$ nuclei is about 1.1 times larger than that of ^{63}Cu for both positions of copper, i.e., the relaxation process is primarily of the magnetic origin.

VI. DISCUSSIONS

A. NQR frequencies

As already mentioned, the copper NQR spectrum of CuS is typical for two crystallographically nonequivalent positions of copper (Figs. 2 and 3). Actually, covellite CuS is constructed from two different Cu complexes: the triangular $[\text{Cu}(1)\text{-S}(1)_3]$ one and the tetrahedral $[\text{Cu}(2)\text{-S}(1)_1\text{S}(2)_3]$ one (Fig. 1). The analysis of NMR spectra has shown that the high-frequency satellite lines (ν_Q was estimated to be ~ 14.7 MHz) are assigned to three-coordinated Cu(1), whereas the low-frequency satellite lines ($\nu_Q \sim 1.5$ MHz) are attributed to four-coordinated Cu(2).^{15,27} Thus, the experimentally observed ^{63}Cu NQR signals at 14.88 MHz (Fig. 2 and Refs. 26–28) and 1.87 MHz (Fig. 3) prove these results.

On the other hand, let us point out the study of a series of copper sulfides, which displays the experimental dependence of the ^{63}Cu quadrupole frequency, ν_Q , on the geometry of the Cu coordination environment.⁵⁹ In particular, in compounds with triangular complexes, CuS_3 , the value of ν_Q lies within the range of 20–25 MHz, whereas for the tetrahedral coordination, CuS_4 , ν_Q either equals zero (regular tetrahedron) or is small (distorted tetrahedron), usually less than 3 MHz. The theoretical calculations of EFG on Cu sites in CuS_3 units, carried out by the Mulliken-Wolfsberg-Helmholtz technique, demonstrate a good agreement of the computed values with the experimental data, for example, in ternary sulfide Cu_3BiS_3 (wittichenite).⁶⁰ It was shown that EFG [see Eq. (5)] is mainly formed by the lattice term (90%), and at less extent, by Cu-3d and Cu-4p orbitals (altogether 10%). A quite narrow range of the ν_Q changes in these sulfides can be explained by insignificant variations in the Cu-S distances, S-Cu-S angles, and the polarity of chemical bonds.

In this sense, the shift of the NQR frequency ν_Q of triangular copper Cu(1) in CuS toward the lower values by about 5 MHz appears rather essential and unusual. This result indicates the relevance of the valence contribution for the EFG

at the Cu(1) site. We suggest that the origin of the ν_Q lowering is correlated with anomalously short Cu(1)-S distances in CuS compared to those in other sulfides (Sec. II) and related to the charge transfer between Cu-4*p*, 3*d* and S-3*p* orbitals. In fact, in a number of cases the reduction in metal-ligand distances leads to the stronger hybridization of chemical bonds with subsequent charge transfer and its redistribution between different orbitals, which can decrease the total EFG and ν_Q values.⁵⁵ The delafossite-based copper oxides CuMO₂ (*M*=Fe, Al, Ga) may serve as an example of such behavior.⁶¹ It was illustrated that the reduction in only one Cu-O distance in linear CuO₂ units from 2.00 Å (CuAlO₂) down to 1.84 Å (CuGaO₂) leads to a decrease in electronic density of the Cu-4*p_z* orbital and an increase in population of Cu-4*p_x* and Cu-4*p_y* orbitals, which play a key role in the experimentally observed lowering of the total EFG value at the Cu site by about 1.5 MHz [Eq. (7b)]. Since the O and S atoms have identical electronic configurations of outer shells (2*s*²2*p*⁴ and 3*s*²3*p*⁴, respectively), it is logical to suppose that somewhat similar mechanism of the ν_Q lowering takes place in CuS. It is not excluded that in the same manner the ν_Q lowering can be also caused by the charge redistribution in Cu-3*d* orbitals [Eq. (7a)]. The influence of the charge transfer on the relaxation and Cu valence is discussed below.

Significant deformations of the CuS₄ tetrahedron break the cubic symmetry, and as was mentioned, EFG on the copper nucleus in this position becomes nonzero. Evidently, this case is realized for the tetrahedral Cu(2) sites in CuS (Fig. 3). Therefore, our NQR spectra prove the crystallographic data²⁴ concerning the occurrence of low-symmetry distortions around Cu(2) sites below T_{PT} [Fig. 1(b) and Table I]. It is an independent confirmation of the low-*T* model of the CuS structure. The laborious search for a possible low-frequency NQR signal at $T=77$ K (above T_{PT}) found no traces indicating that the ν_Q value would be less than 1.5 MHz (technical limit of our NQR spectrometer). Indeed, the estimation of ν_Q for Cu(2) using Eq. (6) for the room-*T* modification (Table I) predicts the values of about 0.4 MHz, which signifies the negligible distortions of Cu(2)S₄ at $T>55$ K.

B. Knight shift

Before analyzing the experimental nuclear relaxation behavior and copper valence, it is expedient to comment on intriguing NMR data in CuS.¹⁵ The Cu NMR studies have shown that the Knight shift *K* for Cu(1) has a significant negative value (−1.4% at 15 K) but the explanation concerning the origin of such anomalous shift was not given. The total Knight shift for transition-metal compounds can be expressed as $K=K_s+K_{orb}+K_d(T)$, where only $K_d(T)$ is negative and depends on *T*.^{58,62,63} Other contributions to total *K* are considered to be negligible.⁶² The first term K_s arises from the contact interaction of nuclear magnetic moments with spin-carrying electrons in the *s* band and reflects the *s*-character Fermi-level density of states (DOS). The second term K_{orb} is the shift originating from the orbital motion of electronic charges. The third term K_d is created due to the exchange interaction between *s* electrons and unpaired *d* electrons (referred to as “core-polarization” effect) and re-

lated to the hybridization with *d* electrons.^{58,64} In some cases, the significant exchange polarization of *s* states by *d* states can generally contribute to the negative total shift *K*,^{58,62} as it takes place, for instance, in ternary carbides M_2AlC (*M*=Ti, V, Cr).⁶⁴ Evidently, K_d overcomes the contribution from positive K_s and K_{orb} in CuS, leading to the negative total shift. Thus, the observed *K* clearly reveals the enhancement of *p-d* hybridization between Cu-3*d* and S-3*p* orbitals. Such a result has been found to be consistent with that expected from theoretical calculations,³⁵ indicating that *p-d* hybridization is substantial and that the ionic models (Cu¹⁺)₃(S₂^{−2})(S^{−1}) or (Cu¹⁺)₃(S₂^{−1})(S^{−2}) appear to be rather oversimplified.

C. Copper nuclear relaxation and Fermi-level density of state

Conduction electrons are known to govern the nuclear spin-lattice relaxation in metallic crystals.^{58,62,63} The *T* dependence of the relaxation rate T_1^{-1} in this case is determined by fluctuations of the hyperfine magnetic field or the EFG with the frequencies $\sim 10^{15}$ s^{−1} created by the conducting electron charges at the nucleus site.^{65,66} The isotopic ratio of Cu relaxation rates emphasizes the magnetic character of fluctuations (Sec. V C). In the approach of free isotropic electronic gas and under the assumption that fluctuating magnetic fields are produced by the contact interaction of a nucleus with the *s*-band electrons, the relaxation can be expressed as $T_1^{-1}=CTN(E_F)\langle|\Psi(0)|^2\rangle_F$, where *C* is a constant, $\langle|\Psi(0)|^2\rangle_F$ is the electronic spin density at the nucleus, and $N(E_F)$ represents the DOS of *s*-band electrons at the Fermi level, $N_s(E_F)$.⁶² Since all these parameters are independent of *T*, a lot of metals exhibit the well-known constant T_1T behavior. Actually, the constant T_1T holds approximately above $T_{PT}=55$ K (Fig. 5). On the other hand, if the core-polarization effect becomes significant in transition metals (Sec. VI B), it is quite appropriate to associate the observed T_1 with an effective value of $N(E_F)=N_s(E_F)+N_d(E_F)$, where $N_d(E_F)$ is the *d*-like contribution to DOS.⁶²

At about $T_{PT}=55$ K, the relaxation rate demonstrates a surprising crossover from the constant relation to unusual *T*-dependent T_1T behavior (Fig. 5), in spite of the fact that CuS appears to be a metal down to $T_c\approx 1.6$ K. Let us summarize the features that characterize the low-*T* electronic behavior.

First, we have checked the *T* dependences of $1/^{63}T_1$ and $1/^{63}T_1T$ in sample 2 and found that data are identical to those in sample 1. Furthermore, earlier studies of the nuclear relaxation for Cu(1) in CuS also supply data for deviations from linearity in $1/^{63}T_1T$ below T_{PT} (Ref. 27) but with no attention paid to such behavior. The identical results for different CuS samples indicate that the observed low-*T* features in relaxation are intrinsic in nature, i.e., they are not associated with any magnetic impurities or lattice defects.

Second, although we do not have conclusive evidence concerning the origin of the unusual T_1T behavior, the following observation suggests that collective electronic motion below T_{PT} is important. Both nonequivalent sites of Cu exhibit a very similar dependence of relaxation on *T*, which gives the constant ratio of the two relaxation times

${}^{\text{Cu}(1)}T_1/{}^{\text{Cu}(2)}T_1 \approx 1.2$ (Fig. 5). Since, in any case, the nuclear relaxation is governed by conduction charges, our result implies the common electronic dynamics for the two non-equivalent Cu(1) and Cu(2), i.e., they “feel” not the individual but the same conduction band. Therefore, taking into account the 2D character of conductivity in CuS below T_{PT} in the direction perpendicular to the c axis (Sec. II), we can suggest that the electronic charges are delocalized not only in the plane of $[\text{Cu}(1)\text{-S}(1)_3]$ units as “the two-dimensional sea”³⁵ but also between two sites of copper, Cu(1) and Cu(2), through the bridging S(1) ion, creating in such a way the “waves” in this sea.

Third, the similar deviations of $1/{}^{63}\text{T}_1T$ from linearity at $T > T_c$ are well known for layered HTSC, in particular, $\text{YBa}_2\text{Cu}_3\text{O}_{6+x}$.^{67,68} Since in usual metals $1/{}^{63}\text{T}_1T \sim [N(E_F)]^2$, a significant decrease in $1/{}^{63}\text{T}_1T$ is widely explained by a decrease in $N(E_F)$. This effect is often referred to as an opening of a “gap” or “pseudogap” in the normal-state DOS. The appearance of such pseudogap in HTSC is also reflected in angle-resolved photoemission spectroscopy (ARPES) and scanning tunneling microscopy (STM) studies.^{67,68} It looks like an analogous deviation of $1/{}^{63}\text{T}_1T$ from the constant value in CuS (Fig. 5) points to the occurrence of some gap in this material below T_{PT} . Therefore, the detailed studies of CuS by ARPES and STM would be expedient. We also add here that interpretations of the pseudogap state in HTSC and its influence on superconductivity are manifold,⁶⁸ including a CDW model.⁶⁹ According to this approach, the pseudogap transformations of electronic spectra take place due to strong scattering of electrons on CDW.

Fourth, the upturn of $1/{}^{63}\text{T}_1T$ for both Cu(1) and Cu(2) below 8 and 16 K, respectively, suggests the presence of a gapless mode. Its origin is not clear for us but similar behavior of relaxation in some HTSC is also observed.⁷⁰

Fifth, it should be noted that $1/{}^{63}\text{T}_1T$ for Cu(1) demonstrates the bends at about 4 and 17 K (Fig. 5), which, most likely, signify the occurrence of some changes in internal dynamics in CuS. Interestingly, these points become apparent also in the heat-capacity³⁷ and ac magnetic-susceptibility¹¹ measurements.

D. Copper valence and charge-density waves

An important piece of information that can be extracted from the NQR spectra data is the absence of magnetic ordering in CuS down to low T . In fact, $1\mu_B$ of the spin moment in $3d$ magnetically ordered state typically gives rise to the strong static field, which would magnetically broaden, split, or shift the NQR lines as it does for the Cu signal in antiferromagnets, $\text{YBa}_2\text{Cu}_3\text{O}_{6+x}$.⁷¹ A sharp single line for each NQR transition of Cu (Sec. V A) and quadrupole character of the line broadening for both ${}^{63}\text{Cu}$ NQR signals (Sec. V B) indicate the absence of the internal static field in CuS in the temperature range studied. This conclusion is in agreement with EPR studies of CuS, showing no paramagnetic divalent Cu^{2+} signal down to low T ,²³ which can suggest the mixed-valence state of Cu besides Cu^{1+} .²³

Actually, NQR can be observed for paramagnetic copper compounds whose linewidths are narrowed due to superex-

change interaction between Cu ions via a bridging ligand.⁷² Particularly, such situation takes place for CuBr_2 , CuCl_2 , and $\text{Cu}_{12}\text{As}_4\text{S}_{13}$.⁷²⁻⁷⁴ The total number of Cu- $3d$ electrons for these materials, n_d , changes between 9.0 (corresponds to paramagnetic Cu^{2+} and electronic spin $S=1/2$) and 10.0 (diamagnetic Cu^{1+} and $S=0$).⁷⁵ In fact, on the basis of Cu- $2p$ XPS studies of CuS, it was estimated that the n_d value can differ from 10.0 but is larger than 9.5.⁷⁵ We turn to the negative shift K_d for Cu(1) (Sec. VI B); this contribution is proportional to the number of unpaired $3d$ electrons.^{58,62} Indeed, the presence of unpaired d electrons was proposed earlier in other studies.⁷⁶ This strongly advocates that Cu is not monovalent in CuS. Therefore, we can suggest that the valence of copper in CuS has a noninteger value and intermediates in the range between Cu^{1+} and $\text{Cu}^{1.5+}$. This is consistent with the interpretation of some crystal-chemical features of CuS,²¹ according to which the valence of Cu(1) and Cu(2) should satisfy the value of $\text{Cu}^{1.3+}$.

Let us now consider the dynamic effects. Theoretical calculations of the CuS conduction band predict that “an electronic charge should flow from the $4t_2$ orbital on the tetrahedral Cu(2) to the $4e$ orbital on the triangular Cu(1)” through the bridging S(1).⁷⁷ Our relaxation studies strongly support this suggestion (Sec. VI C). Moreover, it is proposed that because of the fast charge mobility this electronic transfer can be realized as Cu valence fluctuations.⁴⁵

It has been argued that the T dependence of the NQR frequency ${}^{\text{Cu}(1)}\nu_Q$ in CuS can be understood in terms of charge fluctuations in Cu(1)-S(1)-Cu(2) bonds. It is known that in most noncubic metals $\nu_Q(T)$ can be well reproduced by the empirical Eq. (8) with $b=1.5$; this relation is often referred to as the “ $T^{3/2}$ law.”⁵⁴ Thermal vibrations of the host-lattice atoms are regarded as mainly responsible for such universal relation. However, CuS shows the change in the slope in $\nu_Q(T)$ near 210 K, which exhibits another relation—parameter b in Eq. (8) is close to 1 (notably, according to Ref. 24 the x-diffraction reflections, which become split below T_{PT} , are already broadened at some 150–200 K). In our opinion, the $\nu_Q(T)$ dependence can be better described by two linear functions (Sec. V B). But in any case ${}^{\text{Cu}(1)}\nu_Q(T)$ in CuS does not follow the $T^{3/2}$ law. In this context it is interesting to consider the studies of the mixed-valence metal EuCu_2Si_2 ,⁷⁸ for which the negative Cu Knight shift has been also found.⁷⁹ It was shown that emitting a conduction electron by neighboring Eu ion causes the fluctuation between two electronic configurations of the ion. Such valence instability influences the Cu quadrupole interactions (V_{ZZ}), and as a consequence, the $T^{3/2}$ law becomes invalid. Since in the range of 60–290 K there are no structural changes in CuS (Ref. 24) and $\eta \approx 0$ (Table II), the T dependence of ${}^{\text{Cu}(1)}\nu_Q$ is determined only by V_{ZZ} . Therefore, by analogy, we suggest that the bridging S(1) ion can provide a minor charge transfer between Cu(1) and Cu(2) in some fluctuating regime. The strong hybridization of Cu(1) and Cu(2) conduction bands should allow this transfer (see Secs. VI A–VI C).

It is exciting that our NQR measurements on “plane” Cu(1) in CuS strongly resemble the NQR studies performed on the Cu plane sites in HTSC $\text{YBa}_2\text{Cu}_3\text{O}_7$.⁸⁰ A sharp increase in the NQR linewidth and decay of $1/{}^{63}\text{T}_1T$ led the authors to the conclusion that the charge modulation in the

form of CDW takes place in this material. In general, the CDW comes from the periodic redistribution of electronic charges due to small ionic movement near their equilibrium position in the crystal lattice. In the case of quasi-2D (layered) materials CDWs are formed below some critical temperature and manifest themselves in the appearance of an energy gap in electronic spectra on overlapping Fermi-surface patches (i.e., partial loss of metallic properties) and DOS modulations. Actually, the plane Cu(1) ions have a large anisotropic thermal motion (Sec. II), and strange oscillations of cross sections of the Fermi surface have been detected.²⁵ Thus, the similarity of NQR data allows us to suppose that CDW can exist in CuS and that CDWs manifest themselves as a divergence of $1/^{63}\text{T}_1T$ from the constant value below T_{PT} and unusual $\nu_Q(T)$ dependence.

The “pure” NQR studies of layered dichalcogenides are relatively rare, and it is difficult to compare our NQR results in CuS with those in other dichalcogenides. It is known that low- T superconductor NbSe₂, in which the presence of CDW is proved,¹⁷ also demonstrates an unusual $^{\text{Nb}}\nu_Q(T)$ dependence.⁸¹

E. Phase transition in CuS

The comparison of the ^{63}Cu NQR spectrum for CuS (Figs. 2 and 3) and the ^{63}Cu NQR spectrum for selenium analog of CuS, α -CuSe (klockmannite),⁸² can highlight some reasons for PT. It was found that α -CuSe is characterized by 13 lines in the spectrum with NQR frequencies in the range of 12.7–2.09 MHz at 4.2 K. This points to the presence of strong deformations of the α -CuSe crystal and gives evidence that CuS and α -CuSe are not isostructural as was supposed earlier.⁸³

It is clearly seen that insertion of Se atoms instead of S in CuS results in the conversion of Cu(1) threefold units into distorted fourfold ones (since ^{63}Cu NQR frequencies are rather low) and that α -CuSe has at least 13 nonequivalent Cu positions. In our opinion, the preferential occupation of Se at the S(2) sites³⁸ leads to the approaching of some Se(2) atoms to Cu(1) sites and to the formation of “new” distorted tetrahedrons [Cu(1)-Se(1)₃Se(2)₁] in CuSe instead of “old” triangular units [Cu(1)-S(1)₃] in CuS (Fig. 1). In this case such deformations would promote the approaching of Cu(1) and Cu(2) ions to each other and creation of an effective interaction between them, as was proposed for CuS and α -CuSe.^{24,84} Upon cooling this interaction can stimulate the hexagonal-to-orthorhombic transition.^{24,84} Such scenario is supported by the dependence of the T_{PT} value on the Se amount in mixed samples of $\text{CuS}_{1-x}\text{Se}_x$ ($0 \leq x \leq 1$).³⁸ Actually, since the Cu(1)-Cu(2) bonds in CuS are longer than that in $\text{CuS}_{1-x}\text{Se}_x$, this PT in CuS occurs at lower T .

VII. CONCLUSIONS

We have studied the electronic behavior of 2D transition-metal CuS (covellite) using NQR as a probe in a wide tem-

perature range. We have found that synthetic and natural CuS exhibit not one but two ^{63}Cu NQR signals at 1.87 and 14.88 MHz (4.2 K), which are attributed to Cu(2) and Cu(1) nuclei, respectively. The pure NQR spectra in CuS are an experimental proof that no magnetic ordering occurs in this compound. The direct observation of the low-frequency ^{63}Cu NQR signal in CuS demonstrates serious distortions of the [Cu(2)-S₄] units at low temperatures. The high-frequency ^{63}Cu NQR signal is shifted from the frequency range of 20–25 MHz typical for three-coordinated Cu by S atoms in other copper sulfides, and therefore, this serves as an indication of the strong hybridization of Cu(1)–S(1) bonds. The temperature dependences of the Cu(1) quadrupole frequency ν_Q , linewidth $\Delta\nu_Q$, and nuclear spin-lattice relaxation T_1 altogether display the occurrence of a structural phase transition at about 55 K. It has been argued that this transition is stimulated by Cu(1)-Cu(2) interactions. An unusual behavior of the nuclear relaxation rates of Cu(1) and Cu(2) provides evidence that this phase transition is accompanied by electronic spectra transformations, which could be interpreted as the formation of an energy gap. Moreover, the nuclear relaxation rates of both Cu ions point to the strong hybridization of Cu(1) and Cu(2) conduction bands through S(1) orbitals, leading to the presence of the charge transfer in Cu(1)-S(1)-Cu(2) bonds even in the low- T anisotropic 2D regime. The low- T relaxation of ^{63}Cu is also indicative of a significant contribution of d density of states at the Fermi level. The analysis of the NQR spectra and literature data allows us to conclude that the valence state of both Cu(1) and Cu(2) is not strictly monovalent Cu^{1+} or divalent Cu^{2+} but is intermediate $\text{Cu}^{1.3+}$. In addition, the dependence of the Cu(1) quadrupole frequency ν_Q on T , which is not typical for “simple” metals, has been interpreted from a viewpoint of the Cu valence fluctuations in the vicinity of the average value. We have suggested that charge-density waves in the CuS electronic structure could be responsible for the appearance of the energy gap and may be connected to the charge transfer and Cu valence instability. Nevertheless, the detailed microscopic picture of this phenomenon is unclear at present.

Finally, our results clearly show that CuS exhibits interesting properties and appears to be a good example of the superconductive class of materials. We believe that the reported NQR studies can be considered as a basis for further studies both experimental and theoretical.

ACKNOWLEDGMENTS

Authors express warmest thanks to Eremin M. V. (Kazan State University) for constructive advices. Authors thank Krinari G. A. (Kazan State University) for XRD characterization of the samples and Panarina N. Y. (Kazan Physical-Technical Institute of Zavoisky) for assistance in preparation of the paper. This work is partly supported by the Grant RNP-6183 from the Ministry of Science and Education, Russian Federation.

- *Author to whom correspondence should be addressed. FAX: 7-843-238-72-01; ramil.gainov@ksu.ru
- ¹D. J. Vaughan and J. R. Craig, *Mineral Chemistry of Metal Sulphides* (Cambridge University Press, Cambridge, England, 1978).
 - ²A. S. Marfunin, *Physics of Minerals and Inorganic Materials: An Introduction* (Springer-Verlag, Berlin, 1979); *Physics of Minerals and Inorganic Materials: An Introduction* (Nedra, Moscow, USSR, 1974).
 - ³V. M. Izoitko, *Technological Mineralogy and Estimation of Ore* (Nauka, St. Petersburg, Russia, 1997).
 - ⁴C. I. Pearce, R. A. D. Patrick, and D. J. Vaughan, *Rev. Mineral. Geochem.* **61**, 127 (2006).
 - ⁵See, for example, L. A. Isac, A. Duta, A. Kriza, I. A. Enesca, and M. Nanu, *J. Phys.: Conf. Ser.* **61**, 477 (2007).
 - ⁶See, for example, A. J. Aguiar, C. L. S. Lima, Y. P. Yadava, L. D. A. Tellez, J. M. Ferreira, and E. Montarroyos, *Physica C* **341**, 593 (2000).
 - ⁷J.-S. Chung and H.-J. Sohn, *J. Power Sources* **108**, 226 (2002).
 - ⁸See, for example, W. U. Dittmer and F. C. Simmel, *Appl. Phys. Lett.* **85**, 633 (2004).
 - ⁹W. Meissner, *Z. Phys.* **58**, 570 (1929).
 - ¹⁰W. Buckel and R. Hilsch, *Z. Phys.* **128**, 324 (1950).
 - ¹¹F. Di Benedetto, M. Borgheresi, A. Caneschi, G. Chastanet, C. Cipriani, D. Gatteschi, G. Pratesi, M. Romanelli, and R. Sessoli, *Eur. J. Mineral.* **18**, 283 (2006).
 - ¹²J. G. Bednorz and K. Müller, *Z. Phys. B: Condens. Matter* **64**, 189 (1986).
 - ¹³See, for example, I. R. Mukhamedshin, H. Alloul, G. Collin, and N. Blanchard, *Phys. Rev. Lett.* **94**, 247602 (2005).
 - ¹⁴H. Nozaki, K. Shibata, and N. Ohhashi, *J. Solid State Chem.* **91**, 306 (1991).
 - ¹⁵S.-h. Saito, H. Kishi, K. Nie, H. Nakamaru, F. Wagatsuma, and T. Shinohara, *Phys. Rev. B* **55**, 14527 (1997).
 - ¹⁶R. Könenkamp, *Phys. Rev. B* **38**, 3056 (1988).
 - ¹⁷A. H. Castro Neto, *Phys. Rev. Lett.* **86**, 4382 (2001).
 - ¹⁸A. A. Kordyuk, S. V. Borisenko, V. B. Zabolotnyy, R. Schuster, D. S. Inosov, D. V. Evtushinsky, A. I. Plyushchay, R. Follath, A. Varykhalov, L. Patthey, and H. Berger, *Phys. Rev. B* **79**, 020504(R) (2009).
 - ¹⁹D. W. Shen, B. P. Xie, J. F. Zhao, L. X. Yang, L. Fang, J. Shi, R. H. He, D. H. Lu, H. H. Wen, and D. L. Feng, *Phys. Rev. Lett.* **99**, 216404 (2007).
 - ²⁰H. Barath, M. Kim, J. F. Karpus, S. L. Cooper, P. Abbamonte, E. Fradkin, E. Morosan, and R. J. Cava, *Phys. Rev. Lett.* **100**, 106402 (2008).
 - ²¹H. T. Evans, Jr. and J. A. Konnert, *Am. Mineral.* **61**, 996 (1976).
 - ²²J. A. Tossell, *Phys. Chem. Miner.* **2**, 225 (1978).
 - ²³K. Bente, *Mineral. Petrol.* **36**, 205 (1987).
 - ²⁴H. Fjellvåg, F. Grønvold, S. Stølen, A. F. Andresen, R. Müller-Käfer, and A. Simon, *Z. Kristallogr.* **184**, 111 (1988).
 - ²⁵W. Liang and M.-H. Whangbo, *Solid State Commun.* **85**, 405 (1993).
 - ²⁶R. S. Abdullin, V. P. Kal'chev, and I. N. Pen'kov, *Sov. Phys. Dokl.* **294**, 1439 (1987).
 - ²⁷Y. Itoh, A. Hayashi, H. Yamagata, M. Matsumura, K. Koga, and Y. Ueda, *J. Phys. Soc. Jpn.* **65**, 1953 (1996).
 - ²⁸H. Tnabe, H. Kishi, Nakamaru, S.-h. Saito, F. Wagatsuma, and T. Shinohara, *Meet. Abstr. Phys. Soc. Japan* **52**, 710 (1997).
 - ²⁹L. G. Berry, *Am. Mineral.* **39**, 504 (1954) and reference therein.
 - ³⁰A. S. Povarenikh, *Crystal Chemical Classification of Minerals* (Plenum, New York, 1972); *Crystal Chemical Classification of Minerals* (Naukova Dumka, Kiev, USSR, 1966).
 - ³¹N. V. Belov and E. A. Pobedinskaya, *Kristallografiya* **13**, 969 (1968) [*Sov. Phys. Crystallogr.* **13**, 843 (1969)].
 - ³²R. Kalbskopf, F. Pertlik, and J. Zemann, *Tschermaks Mineral. Petrogr. Mitt.* **22**, 242 (1975).
 - ³³M. Ohmasa, M. Suzuki, and Y. Takeuchi, *Mineral. J.* **8**, 311 (1977).
 - ³⁴A. Putnis, J. Grace, and W. E. Cameron, *Contrib. Mineral. Petrol.* **60**, 209 (1977) and reference therein.
 - ³⁵H. J. Gotsis, A. C. Barnes, and P. Strange, *J. Phys.: Condens. Matter* **4**, 10461 (1992).
 - ³⁶M. Isino and E. Kanda, *J. Phys. Soc. Jpn.* **35**, 1257 (1973).
 - ³⁷E. F. Westrum, Jr., S. Stølen, and F. Grønvold, *J. Chem. Thermodyn.* **19**, 1199 (1987).
 - ³⁸H. Nozaki, K. Shibata, M. Ishii, and K. Yukino, *J. Solid State Chem.* **118**, 176 (1995).
 - ³⁹M. Ishii, K. Shibata, and H. Nozaki, *J. Solid State Chem.* **105**, 504 (1993).
 - ⁴⁰T. Nakajima, M. Isino, and E. Kanda, *J. Phys. Soc. Jpn.* **28**, 369 (1970).
 - ⁴¹T. Chattopadhyay and A. R. Chetal, *J. Phys. Chem. Solids* **46**, 427 (1985).
 - ⁴²M. Grioni, J. B. Goedkoop, R. Schoorl, F. M. F. de Groot, J. C. Fuggle, F. Schäfers, E. E. Koch, G. Rossi, J.-M. Esteve, and R. C. Karnatak, *Phys. Rev. B* **39**, 1541 (1989).
 - ⁴³I. B. Borovskii and I. A. Ovsyannikova, *Zh. Eksp. Teor. Fiz.* **37**, 1458 (1959) [*Sov. Phys. JETP* **37**, 1033 (1959)].
 - ⁴⁴L. Nakai, Y. Sugitani, K. Nagashima, and Y. Niwa, *J. Inorg. Nucl. Chem.* **40**, 789 (1978).
 - ⁴⁵J. C. W. Folmer and F. Jellinek, *J. Less-Common Met.* **76**, 153 (1980).
 - ⁴⁶D. L. Perry and J. A. Taylor, *J. Mater. Sci. Lett.* **5**, 384 (1986).
 - ⁴⁷G. van der Laan, R. A. D. Patrick, C. M. B. Henderson, and D. J. Vaughan, *J. Phys. Chem. Solids* **53**, 1185 (1992).
 - ⁴⁸R. A. D. Patrick, J. F. W. Mosselmans, J. M. Charnock, K. E. R. England, G. R. Helz, C. D. Garner, and D. J. Vaughn, *Geochim. Cosmochim. Acta* **61**, 2023 (1997).
 - ⁴⁹S. W. Goh, A. N. Buckley, R. N. Lamb, R. A. Rosenberg, and D. Moran, *Geochim. Cosmochim. Acta* **70**, 2210 (2006).
 - ⁵⁰E. Z. Kurmaev, J. van Ek, D. L. Ederer, L. Zhou, T. A. Callcott, R. C. C. Perera, V. M. Cherkashenko, S. N. Shamin, V. A. Trofimova, S. Bartkowski, M. Neumann, A. Fujimori, and V. P. Molosha, *J. Phys.: Condens. Matter* **10**, 1687 (1998).
 - ⁵¹D. Li, G. M. Bancroft, M. Kasrai, M. E. Fleet, X. H. Feng, B. X. Yang, and K. H. Tan, *Phys. Chem. Miner.* **21**, 317 (1994).
 - ⁵²C. Sugiura, H. Yamasaki, and S. Shoji, *J. Phys. Soc. Jpn.* **63**, 1172 (1994).
 - ⁵³A. P. Bussandri and M. J. Zuriaga, *J. Magn. Reson.* **131**, 224 (1998).
 - ⁵⁴E. N. Kaufmann and R. J. Vianden, *Rev. Mod. Phys.* **51**, 161 (1979).
 - ⁵⁵G. K. Semin, T. A. Babushkina, and G. G. Yakobson, *Nuclear Quadrupole Resonance in Chemistry* (Wiley, New York, 1975); *Nuclear Quadrupole Resonance in Chemistry* (Khimiya, Leningrad, USSR, 1972).
 - ⁵⁶J. L. K. F. De Vries, C. P. Keijzers, and E. De Boer, *Inorg. Chem.* **11**, 1343 (1972).
 - ⁵⁷Itoh (Ref. 27) studied the $^{Cu(1)}\nu_Q(T)$ with small amount of steps within 100–300 K, whereas Tnabe (Ref. 28) measured the value

- of $\text{Cu}^{(1)}\nu_Q$ only up to 80 K. Therefore the bend of $\nu_Q(T)$ at 210 K in these studies is not found.
- ⁵⁸J. Winter, *Magnetic Resonance in Metals* (Clarendon, Oxford, 1971).
- ⁵⁹R. S. Abdullin, V. P. Kal'chev, and I. N. Pen'kov, *Phys. Chem. Miner.* **14**, 258 (1987); V. P. Kal'chev, Ph.D. thesis, Kazan State University, 1988.
- ⁶⁰I. N. Pen'kov, R. S. Abdullin, N. B. Yunusov, and N. V. Togulev, *Izv. Akad. Nauk SSSR, Ser. Fiz.* **42**, 2104 (1978) [*Bull. Acad. Sci. USSR, Phys. Ser.* **42**, 2104 (1978)].
- ⁶¹R. S. Abdullin, I. N. Pen'kov, and N. B. Yunusov, *Izv. Akad. Nauk SSSR, Ser. Fiz.* **45**, 1787 (1981) [*Bull. Acad. Sci. USSR, Phys. Ser.* **45**, 1787 (1981)].
- ⁶²A. Narath, in *Hyperfine Interactions*, edited by A. J. Freeman and R. B. Frenkel (Academic, New York, 1967).
- ⁶³C. P. Slichter, *Principles of Magnetic Resonance* (Springer-Verlag, Berlin, 1996).
- ⁶⁴C. S. Lue, J. Y. Lin, and B. X. Xie, *Phys. Rev. B* **73**, 035125 (2006).
- ⁶⁵A. H. Mitchell, *J. Chem. Phys.* **26**, 1714 (1957).
- ⁶⁶A. R. Kessel, *Fiz. Met. Metalloved.* **23**, 837 (1967) [*Phys. Met. Metallogr.* **23**, 837 (1967)].
- ⁶⁷N. M. Plakida, *High-temperature Superconductivity* (Springer-Verlag, Berlin, 1995); D. Brinkmann, *J. Mol. Struct.* **345**, 167 (1995).
- ⁶⁸M. V. Sadovskii, *Phys. Usp.* **44**, 515 (2001).
- ⁶⁹A. V. Dooglav, M. V. Eremin, Yu. A. Sakhratov, and A. V. Savinkov, *JETP Lett.* **74**, 103 (2001); M. V. Eremin, I. Eremin, and A. Terzi, *Phys. Rev. B* **66**, 104524 (2002).
- ⁷⁰K. Ishida, K. Yoshida, T. Mito, Y. Tokunaga, Y. Kitaoka, K. Asayama, A. Nakayama, J. Shimoyama, and K. Kishio, *Phys. Rev. B* **58**, R5960 (1998).
- ⁷¹A. V. Dooglav, H. Alloul, M. V. Eremin, and A. G. Volodin, *Physica C* **272**, 242 (1996).
- ⁷²T. J. Bastow, I. D. Campbell, and K. J. Whitfield, *Solid State Commun.* **33**, 399 (1980).
- ⁷³R. R. Gainov, A. V. Dooglav, and I. N. Pen'kov, *Solid State Commun.* **140**, 544 (2006).
- ⁷⁴R. R. Gainov, A. V. Dooglav, I. N. Pen'kov, I. R. Mukhamedshin, A. V. Savinkov, and N. N. Mozgova, *Phys. Chem. Miner.* **35**, 37 (2008).
- ⁷⁵C. I. Pearce, R. A. D. Patrick, D. J. Vaughn, C. M. B. Henderson, and G. van der Laan, *Geochim. Cosmochim. Acta* **70**, 4635 (2006).
- ⁷⁶T. Novakov, *Phys. Rev. B* **3**, 2693 (1971).
- ⁷⁷D. J. Vaughan and J. A. Tossell, *Phys. Chem. Miner.* **9**, 253 (1983).
- ⁷⁸E. V. Sampathkumaran, L. C. Gupta, and R. Vijayaraghavan, *Phys. Rev. Lett.* **43**, 1189 (1979); *J. Mol. Struct.* **58**, 89 (1980).
- ⁷⁹M. Baenitz, A. A. Gippius, A. K. Rajarajan, E. N. Morozova, Z. Hossain, C. Geibel, and F. Steglich, *Physica B* **378-380**, 683 (2006).
- ⁸⁰B. Grévin, Y. Berthier, and G. Collin, *Phys. Rev. Lett.* **85**, 1310 (2000).
- ⁸¹D. R. Torgeson and F. Borsa, *Phys. Rev. Lett.* **37**, 956 (1976).
- ⁸²V. P. Kal'chev, I. N. Pen'kov, and T. A. Kalinina, *Zapiski VMO [Proceedings RMS]* **6**, 81 (1989).
- ⁸³R. D. Heyding and R. M. Murray, *Can. J. Chem.* **54**, 841 (1976).
- ⁸⁴V. Milman, *Acta Crystallogr., Sect. B: Struct. Sci.* **58**, 437 (2002) and reference therein.